Modulation Recognition Using Cyclostationary Heat Maps With Residual/Deep Learning

James Norris, Senior Member IEEE,
Ryan Seeber, and John Nieto
L3Harris Corporation
Rochester, NY
james.norris@l3harris.com ryan.seeber@l3harris.com john.nieto@l3harris.com

***Abstract* – Deep Learning is a commonly used tool for Modulation Detection and Identification. Similarly, cyclostationary analysis has a long history of utility in modulation identification. In this paper a novel application of multiple higher-order cyclostationary heat maps are used in neural network training – replacing Inphase and Quadrature samples that were used in prior work. Several standard modulation types have been identified from standard references – BPSK, QPSK, OFDM, etc. with various attempts made to create the most effective heat maps. The training and validation accuracy is discussed. As SNR decreases, the most effective modulation prediction should select noise rather than modulation and the point at which the neural network switches from each modulation to the noise as a default basis is provided as an enhancement over other ML/AI techniques that simply do not provide noise as a prediction option with the alternate that the network has been confused by an unknown modulation.**

Keywords— AI; ML; Deep Learning; Neural Networks; LPI; LPD; SIGINT; Cyclostationary; Spectral Correlation Function

I. INTRODUCTION

There is a continuing need to improve techniques for detecting and identifying RF signals for many applications which include optimizing spectrum access and collision avoidance, and for electronic surveillance and signal classification. Cognitive radios are a key part of identifying open frequency bands. Many of these frequency bands are allocated for the exclusive use of specific technology comprised of known modulation types of fixed bandwidth. But many (like the military bands for example) can be used for less commonly used, non-commercial, modulation and bandwidth combinations. For both application spaces (surveillance and spectrum access) it is highly desirable to achieve the ability to identify known signals and to be able to train and identify less commonly used signals.

There has been a lot of research related to signal detection and identification using various types of AI/ML models [1]. In this approach a Long Short-Term Memory (LSTM) is an enhancement to a recurrent neural network that has recently shown improvements over a more commonly used convolutional neural network (CNN).

Several techniques are utilized for modulation detection and identification. Time domain techniques utilize captured I&Q samples to train a convolutional neural network using semi-supervised learning [2]. One approach converted the I&Q samples to the frequency domain and performed cyclostationary feature analysis [3] in single-dimensional thresholds on spectral features.

Our novel concepts for this paper are threefold – the first is to replace single-dimension cyclostationary analysis used in prior work with images that simultaneously represent multiple, higher-order cyclostationary results. Secondly, we illustrate that the pre-processing we've used can achieve any desired SNR given that coherent integration is utilized. For our work, we decided that the goal is to utilize the same number of symbols and match the SNR performance from prior work knowing that our coherent integration technique could achieve detection at the desired SNR. Finally, we expand on the library of modulation types recognized by the CNN with the inclusion of Additive White Gaussian Noise. (Note that the images presented in this work do not have x-axis or y-axis labels as they are the actual images presented to the CNN). Our motivation, given the larger library which includes AWGN is to consider spectral adaptation as an application. The decision threshold between a valid modulation signal and AWGN is a critical piece in spectral adaptation as the decision on whether to re-use a portion of that spectrum based on faulty input (from the CNN decision) which could result in over-the-air collisions. This paper analyzes and discusses the tradeoff between a robust AWGN detection as opposed to existing systems which do not provide an identification of noise in the absence of an identification of a known modulation.

I. Spectral Density and Correlation Functions

There are several cyclostationary detection methods described throughout a significant amount of research [3][4][5][6][7][8].

One method of cyclostationary feature analysis is the Spectral Correlation Function (SCF).

$$\frac{1}{T} X_T\left(t, f-\frac{\alpha}{2}\right) X_T^*\left(t, f+\frac{\alpha}{2}\right) \qquad (1)$$

Where X_T is the Fourier Transform of the input *x(t)* signal, X_T^* is the conjugate Fourier transform and α is the spectral shift corresponding to the cyclostationary spectral frequency. Shown in Figure 1 is the SCF of BPSK. The horizontal axis has both a frequency and alpha dimension and the vertical axis is the average of the magnitude squared of each complex FFT bin. For $\alpha = 0$, the SCF displays the standard power spectrum that is expected for BPSK. The energy that appears in the bins where $\alpha \neq 0$ are the cyclostationary features.

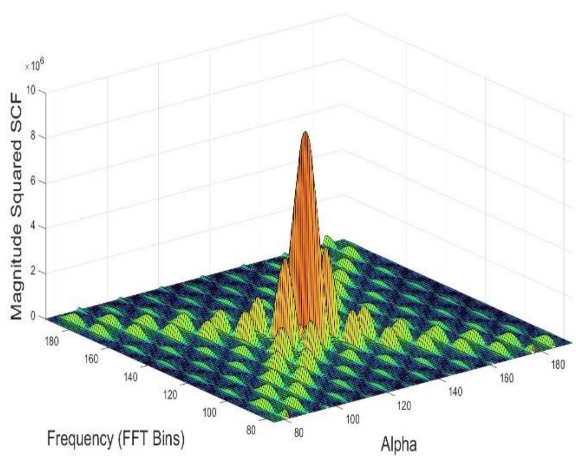

Fig. 1. Spectral Correlation Function of BPSK

The formula for a second-order chip rate detector is shown in equation (2).

$$E[FFT[x(n)x^*(n)]] \qquad (2)$$

Where *x(n)* is the digitally sampled received signal which is squared with the conjugate of the original sample, converted to the frequency domain, and averaged (or filtered in some applications). The resulting 2^{nd} order detector is illustrated in Figure 2.

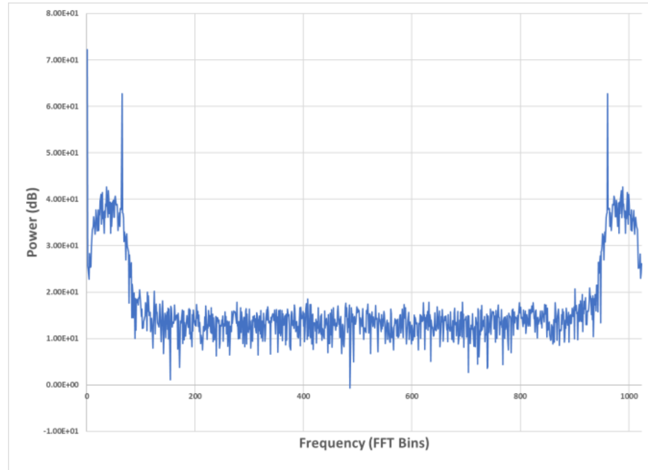

Fig. 2. Spectral Correlation Density of BPSK

More cyclostationary features can be found using a fourth-order Spectral density transformation [9][10] The equation used for the transformation is shown in equation (3). Note that the complex conjugate is utilized for two of the products and the result is noted as [4,2] as shorthand for the [number of products, number of complex conjugate products].

$$E[x(t+\tau_1)x(t+\tau_1)x^*(t+\tau_1)x^*(t+\tau_1)] \qquad (3)$$

Shown in Figure 3 below is a heat map created from successive combinations of products of the simulation created I&Q data (on the y-axis) with the FFT bins (on the x-axis) and the colors representing the magnitude of each FFT bin (from red as the largest magnitude to blue as the lowest magnitude).

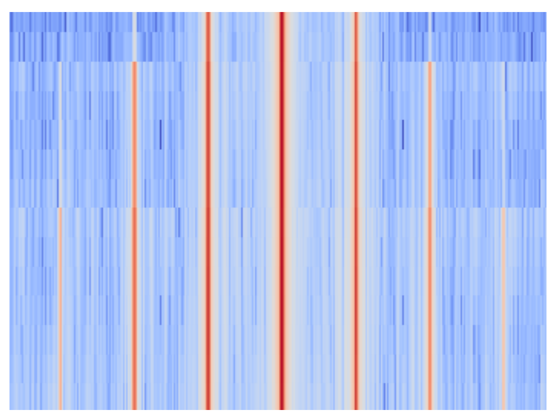

Fig. 3. BPSK Heat Map 20dB SNR

Figure 4 illustrates the advantages of using a coherent integration technique over a time-limited set of training vectors. At -4dB SNR, the noise overwhelms a system with 1000 FFT integrations yet they become clearly visible with 10000 or 100000 integration cycles.

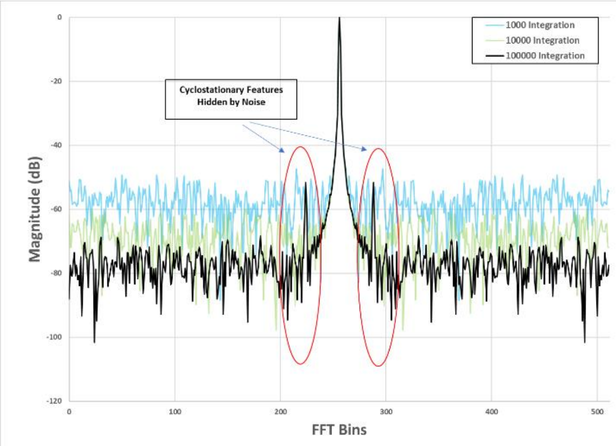

Fig. 4. Illustration of the Effect of Coherent Integration on the Noise Level of a Cyclostationary Analysis

II. AWGN AS A MODULATION TYPE

In previous work, the cyclostationary features of various types of modulation have been characterized and limited to just the prediction probabilities of that modulation as noise is added to the system. In our research, we've included AWGN as a legitimate training type and expect the neural network to switch from the prediction of each modulation to AWGN as the noise level in each pattern increases.

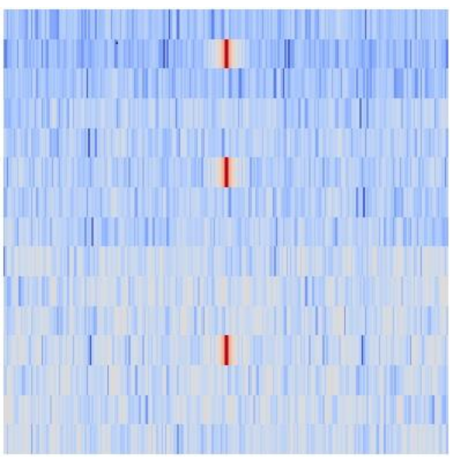

Fig. 5. AWGN Heat Map 10000 Averages

With a convolutional neural network, training requires as many examples of the subject as possible. In this paper, we've created alternate images of noise by altering the amount of averaging collected for each plot. Shown in Figure 5 is the heat map obtained from 10,000 averages. In our training, we've included everything from ten to ten-thousand averages of the cyclostationary spectrum.

III. CONVOLUTIONAL NEURAL NETWORK

For each modulation type, BPSK, QPSK, 8-ary PSK, CPM, – and now including AWGN, the CNN was provided a range of simulated input signal and noise levels from 20dB SNR down to 0dB SNR in 5dB steps to train on. The first nine patterns chosen randomly as input to the CNN is shown in Figure 6.

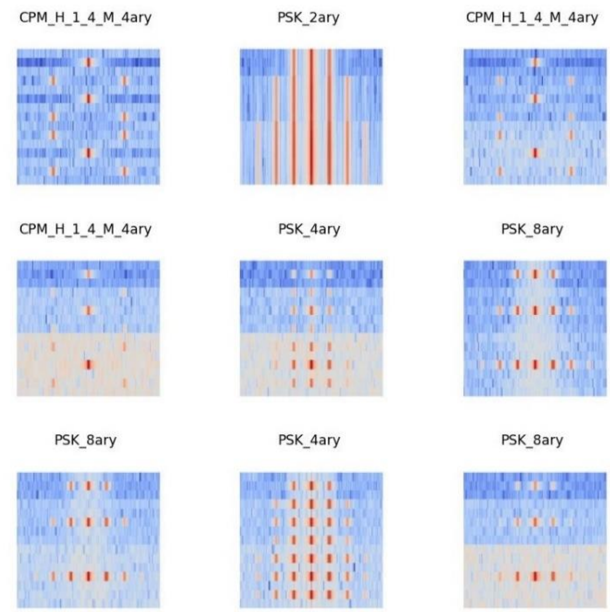

Fig. 6. First Nine Training Patterns used by CNN

Fifty epochs were selected, and the training and validation achieved 100% accuracy within the first 20 epochs. Similarly training and validation loss was at 0% at that same point. At this point, the model was fed with the same modulation types with the SNR ranging from -5dB to -20dB in 1dB steps. The results were encouraging as shown in Table 1.

Table 1. Prediction as a Function of Modulation

Modulation	SNR	Prediction Percentage
BPSK	-9dB	98.79%
QPSK	-4dB	80.12%
8-PSK	0	99.87%
CPM	-8dB	97.55%

The variability in prediction for each of the modulation was unexpected. One of the concerns noted with the heat maps is that the background noise has variable blue and blue-red coloring.

IV. NORMALIZATION OF HEAT MAPS

To improve prediction performance, several attempts were made to reduce the complexity of the images by consolidating the background color (increasing contrast) and to change the distance between the cyclostationary tones (improving resolution).

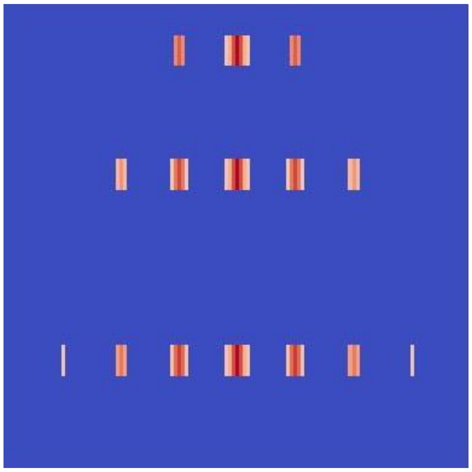

Fig. 7. Hard-Limit Imposed on 8-ary PSK

Resizing the heat map can focus the image on the tones that appear towards the center – expanding their size. It's important to understand that the location of the tones is dependent on the symbol rate of the modulation so this modification can cause the system to miss modulation schemes with higher symbol rates. The background color is homogenized with a hard limit on the ratio of the peak tone to background ratio. The tradeoff with this approach is that some of the tones – including integer multiples of the modulation symbol rate will be eliminated from the image.

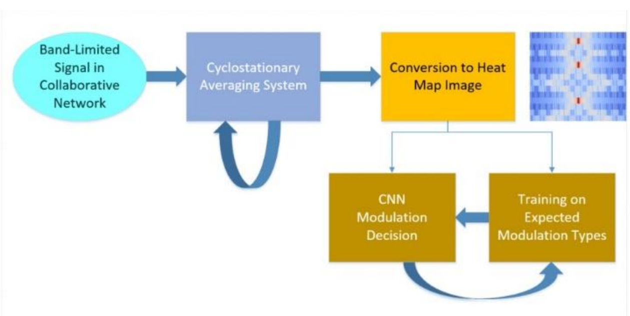

Fig. 8. Spectral Adaptation System Design

V. System Design

In this spectral adaptive system, the primary source of SNR performance comes from successive additions (averages) of the FFT output of the cyclostationary analysis. Thus, the tradeoff to any increase to the amount of coherent averaging is the slower response time in the decision making. That said, the desired maximum range drives the SNR required for the collaborative spectrally adaptive system. For our system analysis, we rely on simulated signals and noise to make sure that the results are reproducible. And our selection for averaging is designed to match the SNR performance of the systems described in the references.

VI. Results

With the addition of the hard-limited and resized images to the training database of the convolutional neural network, predictions improved, and the model was able to correctly identify each modulation type and, when overwhelmed with noise, correctly identify additive white Gaussian noise ('awgn') as illustrated in confusion matrices shown in Figures 9 through 13.

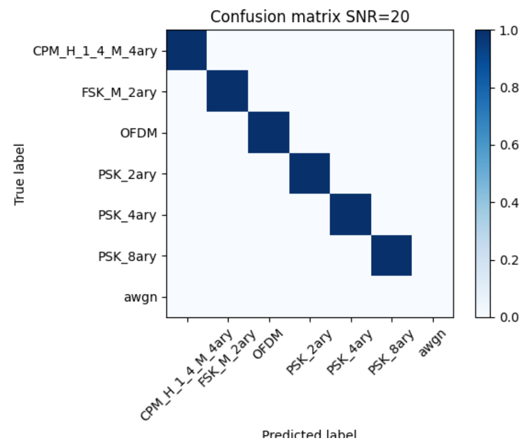

Fig. 9. Modulation Prediction at 20dB SNR

As expected, shown in Figure 9, without any significant noise (Signal/Noise, SNR=20dB), each modulation type is predicted correctly.

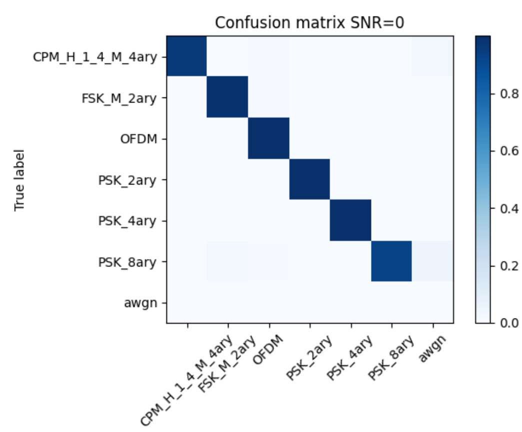

Fig. 10. Modulation Prediction at 0dB SNR

As shown in Figure 10, as noise is increased - all the way to the point where the signal and noise power levels are equivalent (SNR=0dB), the model predicts the correct modulation type.

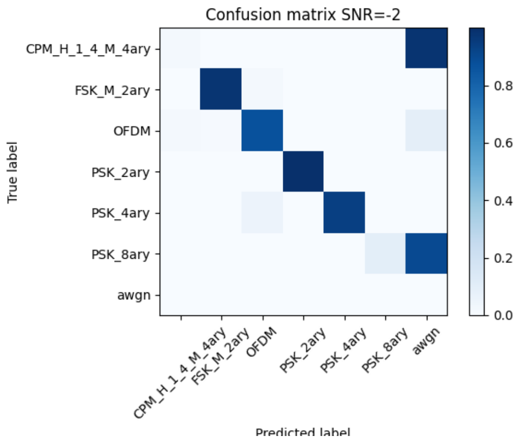

Fig. 11. Modulation Prediction at -2dB SNR

In Figure 11 and 12, once the noise level begins to overwhelm the signal, the model begins to predict noise as the received "signal". This exactly represents what our received system is observing and is accurate.

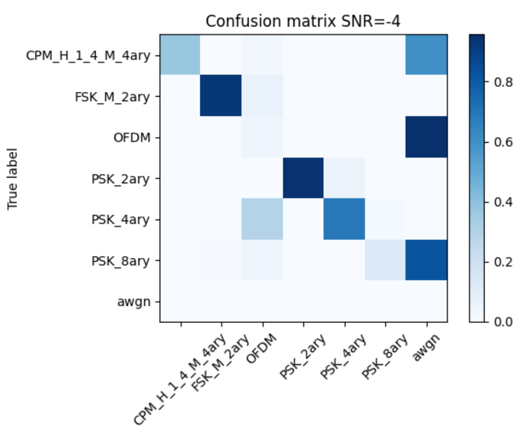

Fig. 12. Modulation Prediction at -4dB SNR

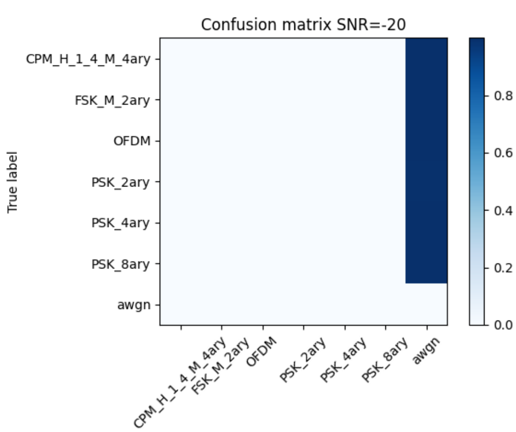

Fig. 13. Modulation Prediction at -20dB SNR

Finally, in Figure 13, when the input signal is completely statistically random, and the cyclostationary tones are not visible in the average spectrum, the model selects 'awgn' as the most likely signal received.

VII. Conclusions

We study the problem of spectral avoidance and modulation recognition for both noise and selected, common modulation types. We create an initial set of images using cyclostationary analysis, train a convolutional neural network, and obtain an initial set of successful predictions. We then create an enhanced set of modulation images and add them to the library for each modulation type to improve predictability of the model. We demonstrated that the complete library of cyclostationary images correctly switch from each modulation type to predicting noise as the signal to noise ratio increases and matches the performance of other published research that limits the predictions to focus on each modulation type.

References

[1] Yanlun Wu, Xingjian Li, and Jun Fang, "A Deep Learning Approach for Modulation Recognition via Exploiting Temporal Correlations", IEEE 19th International Workshop on Signal Processing Advances in Wireless Communications (SPAWC), 2018

[2] Xuezhi He, Lin Lin, and Jinbao Xie, "Radio signals modulation mode recognition based on semisupervised deep learning", IEEE 2nd International Conference on Automation, Electronics, and Electrical Engineering, 2019

[3] A. Fehske, J. Gaeddert and J. H. Reed, "A New Approach to Signal Classification Using Spectral Correlation and Neural Networks", First IEEE International Symposium on New Frontiers in Dynamic Spectrum Access Networks, 2005

[4] Randy S. Roberts; William A. Brown; Herschel H. Loomis, Jr., "Computationally Efficient Algorithms for Cyclic Spectral Analysis" IEEE Signal Processing Magazine, April 1993

[5] Giannakis, G.B. , "Cyclostationary Signal Analysis", Digital Signal Processing Handbook, CRC Press LLC, 1999

[6] Renard, Julien, et. al. "Higher-Order cyclostationarity Detection for Spectrum Sensing" ,EURASIP Journal on Wireless Communications and Networking, Vol. 2010 Article ID 721695

[7] Gardner, William A., Napolitano, Antonio, Paura, Luigi, "Cyclostationarity: Half a Century of Research" Elsevier Computer Science Signal Processing 86 (2006)

[8] Hao Hu, "Cyclostationary Approach to Signal Detection and Classification in Cognitive Radio Systems", Beijing University of Posts and Telecommunications

[9] Octavia A. Dobre, Yeheskel Bar-Ness, Wei Su, "Higher-Order Cyclic Cumulants for High Order Modulation Classification", IEEE Military Communications Conference, MILCOM Oct. 2003

[10] Julien Renard, et. al. , "Higher-Order Cyclostationary Detection for Spectrum Sensing" EURASIP Journal on Wireless Communications and Networking, Volume 2010 Article ID 721695